Construction and Building Materials 238 (2020) 117675

Contents lists available at ScienceDirect

Construction and Building Materials

journal homepage: www.elsevier.com/locate/conbuildmat

Influence of PZT insertion on Portland cement curing process and piezoelectric properties of 0–3 cement-based composites by impedance spectroscopy

J.A. Santos [a], A.O. Sanches [a,*], J.L. Akasaki [a], M.M. Tashima [a], E. Longo [b], J.A. Malmonge [a]

[a] Universidade Estadual Paulista (UNESP), Faculdade de Engenharia, Câmpus de Ilha Solteira. Av. Brasil, 56, 15385-000 Ilha Solteira, SP, Brazil
[b] Universidade Federal de São Carlos–UFSCar, LIEC, Rodovia Washington Luís, s/n, 13565-905 Sãn Carlos, SP, Brazil

HIGHLIGHTS

- Cement cure influence ageing piezoelectric properties.
- Impedance spectroscopy as a function of curing time for 0–3 cement-based piezoelectric composites.
- Cement cure delay by piezoelectric phase.

GRAPHICAL ABSTRACT

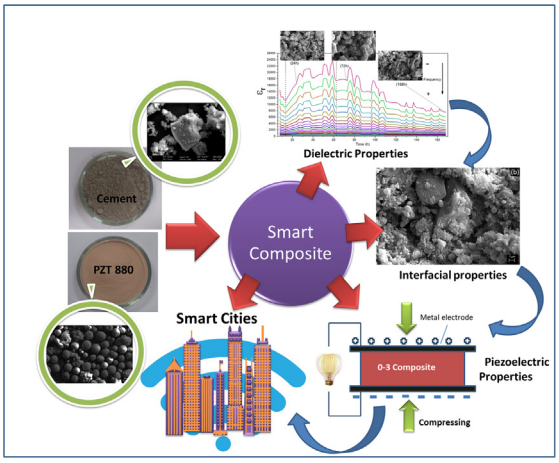

ARTICLE INFO

Article history:
Received 28 August 2019
Received in revised form 19 November 2019
Accepted 22 November 2019
Available online 6 December 2019

Keywords:
Cement-based composites
Impedance spectroscopy
Interface
Sensor

ABSTRACT

0–3 Cement-based piezoelectric composites were produced. It was verified that not only the piezoelectric properties of the composites, but also the influence of piezoelectric phase in the cement paste curing process. The results showed that the final piezoelectric and dielectric properties of the composites depend mainly on the interfacial microstructure between the matrix and the piezoelectric insertion. DC conductivity and impedance spectroscopy measurements showed a high sensitivity to the identification of retard hydration process or phase transformations. Piezoelectric properties show ageing fluctuations, attributed to the cement curing process which promoted unstable dipoles at the same time that it promoted piezoelectric phase constriction.

1. Introduction

With increasing population growth there is also a significant increase in urbanisation. This has been accompanied by the construction of taller buildings, bridges, viaducts, and tunnels for transport, in order to make more efficient use of the increasingly

* Corresponding author.
E-mail address: alex.o.sanches@unesp.br (A.O. Sanches).

https://doi.org/10.1016/j.conbuildmat.2019.117675
0950-0618/

scarce spaces. Since such man-made structures deteriorate over time, a bridge, for example, is designed to have an average life cycle of 60–80 years, the continuous, fast, accurate, and real-time monitoring of such structures is necessary in order to not only to prevent extensive damage, but also, to prevent major accidents. Over the last decades, civil engineering has been moving towards the construction of intelligent structures, in which sensors are arranged on the surface of, or embedded in, such structures, so that healthy monitoring of active vibration control, temperature and lighting, are performed in real time [1-5]. In this sense, piezoelectric sensors have proven to be one of the most efficient for monitoring structural health in the area of civil engineering [5-8]. However, piezoelectric materials commonly used for the sensor's manufacture, such as ferroelectric ceramics and some piezoelectric polymers, do not have good coupling or compatibility with the main material used in construction, concrete [6,7,9]. This behaviour occurs because of the difference in the dielectric constant and acoustic impedance of structural and sensor materials [9]. Trying to overcome such problems, Li et al. [10,11], in 2002, proposed the first study based on the manufacture of biphasic piezoelectric cementitious-composites of 0–3 connectivity. Nowadays, many studies can be found on the use of cement-based piezoelectric composites in the most diverse connectivities, showing the great potential of these composites in applications such as sensors and actuators, not only in the field of civil engineering, but also in the aerospace and other industries. [9,10,12-25]. Although many works have been published about this subject since, compatibility problems, low piezoelectric coefficient and stability problems still persist and are objects of study [9,10,12-25]. Allied to such issues, given the great complexity of the cement curing process, little is known about how the cement curing process interferes in the piezoelectric properties of the active phase, or even how the active phase itself can interfere in the cement curing process. This explains the results variation that can be found in the literature, especially when considering the works based on 0–3 connectivity piezoelectric composites when analyzed quantities/properties as dielectric constant, piezoelectric coefficient (d_{33}), matrix adhesion, aging influence, etc. [6,9,10,20-23,26-32]. Due to this, the current work proposes a study of the influence of the piezoelectric phase on the curing process of the cementitious matrix, and vice versa, based on the impedance spectroscopy technique (EI). As it is a non-destructive and fast response technique, the use of the EI has been increasing in civil engineering for the study of cement pastes and mortars, as well as for the monitoring of curing, corrosion and aging processes concrete-based structures [33-40]. Electrical techniques such as EI have advantages over conventional characterization techniques employed for the study of cement microstructure formation processes, since they exhibit great sensitivity to microstructure formation and change during its curing process [33-35].

This study has as innovation in the fact of showing, that not only the final piezoelectric properties of the composites depend mainly on the interfacial microstructure between the matrix and the piezoelectric insertion, but also, that the introduction of the piezoelectric phase itself directly interferes in the curing process of the matrix.

2. Materials and methods

2.1. Materials

Lead zirconate titanate (PZT) was purchased from APC International Ltd. (Mackeyville, USA) under reference 880. The properties of the PZT ceramic are listed in Table 1. The mean diameter of the PZT particles were obtained by SEM (EVO LS15 - Zeiss) and calculated using ImageJ 1.45 software. About 300 structures were examined (Fig. 2f). CPV-ARI- cement was purchased commercially from Votorantim S.A. under the commercial name Votoran. CPV-ARI- cement composition specified by manufacturer was summarized in the Table 2.

2.2. Composites fabrication

Cement control samples were prepared from a water cement ratio (w/c) = 0.33. For this, the cement was subjected to ball milling (Vibrator DDR-GM 9458) for two minutes. After that, it was mechanically mixed with water for two minutes. The mixture was compacted in circular steel moulds, of 17 mm diameter × 2 mm width, and allowed to dry at 25 °C in ambient atmosphere, for two hours, before unmoulding. Composites were prepared in the proportions of 10, 30, 50 and 70% v/v, maintaining the w/c = 0.33. The samples were produced by mixing the powdered proportions of PZT and cement in a ball mill for two minutes. After that, the same preparation procedure used for the control sample was repeated until unmoulding. The composites samples were designated as CP(X/Y), where X and Y indicate the volume fraction of cement and PZT in the composite, respectively.

2.3. Characterisation

The morphology of the surface and fractured surfaces was evaluated using an EVO scanning electron microscope LS15 - Zeiss. The samples were attached to aluminum stubs with conductive carbon tape and sputtered with gold. The images were collected in backscattering mode (BSD). Electrical conductivity in the DC regime was obtained by the two-probe method using a voltage/current source (Keithley Instruments model 247 high voltage supply). After unmoulding, the samples were metallised with silver paint (MH CONDUX - MY203) and allowed to dry for eight hours, before measurements were started. Measurements were taken every eight hours for seven days, and thereafter, for reference, in 30 days of curing. Voltage was applied to the sample for 10 min and then the current measurement was performed. Three samples were tested for each composition. The mean values were presented here. Dielectric properties of the manufactured composite samples were measured using an SI 1260 Solartron Impedance Analyser with a 1296 Dielectric Interface. The relative dielectric constant (ε_r) was collected in the frequency range of 10^0–10^6 Hz at room temperature. The voltage applied was 1 V. All samples were metallised with silver paint as specified for DC electrical conductivity measurements. The samples dielectric spectra were collected, as a function of the curing time, every hour for seven days. For the d_{33} measurements, the samples were polarised based on curing times in which the cement relative dielectric constant showed a maximum in the dielectric spectrum (Fig. 4). The selected periods were 8, 51, 76 and 130 h, and for final verification, the period of 30 days of curing, which did not produce a ε_r maximum. The polarisations were performed in a silicon oil bath at 90 °C with an electric polarisation field of E = 2 kV/m. Three specimens were polarised for each composition. The d_{33} value was measured at ten positions on each side of each specimen. The mean values are those presented in this work. D_{33} aging values were measured up to 105 days after polarization. Electrical fields above 2 kV/m, at temperatures above 90 °C, promoted the dielectric rupture of the samples for the initial curing periods (8 h). Therefore, for comparison, the value of the polarisation field was standardised for all samples, compatible with the polarisation at all cement cure ages. Fig. 1 summarises the preparation and characterisation steps of the composites.

3. Results

3.1. Scanning electron microscopy

Fig. 2a–e illustrates representative micrographs of the cement and CP(X/Y) composites fractures after 30 days of curing. The presence of small fibrous crystals, characteristic of the hydrated calcium silicate (C-S-H gel), as well as the presence of acicular crystals corresponding to hydrated calcium trisulphoaluminate, known as ettringite (C-A-$\bar{S}$-H), were observed (Fig. 2a–e). PZT can be identified in the composite images by means of its spherical geometry with an average diameter of (78 ± 49) μm (Fig. 2e). For CP (90/10), it was possible to observe the main phases of the composite, composed of PZT grains and the hydration phases C-S-H (Fig. 2a). With the increase of the PZT volumetric fraction, the identification of the cement hydration phases became difficult to assess by microscopic imagery. However, at concentrations up to 30% v/v of PZT, it was still possible to observe the formation of C-S-H, and ettringite (Figure d-e). The images, in general, showed the PZT had a homogeneous distribution, and that this was found in the composite, as a non-reactive phase, due to the low adhesion of cement hydration products around it. Likewise, the increase of the ceramic particulate in the composites promoted the presence of pores, as can be observed. The presence of unhydrated or partially hydrated cement grains can also be observed on microscopy images.

Table 1
Physical, dielectric and piezoelectric properties of PZT 880.

	ε_r (1 kHz)	T_c (°C)	ρ (g/cm^3)	d_{33} (pC/N)	d (μm)
PZT 880	1050	310	7.6	215	78

Table 2
Physical and chemical properties of Portland cement.

SiO_2	Al_2O_3	Fe_2O_3	CaO	MgO	SO_3	L.O.I.	SSA (m^2/g)	Density (g/cm^3)
23.6	6.60	3.09	52.6	5.86	2.26	5.24	1.25	3.14

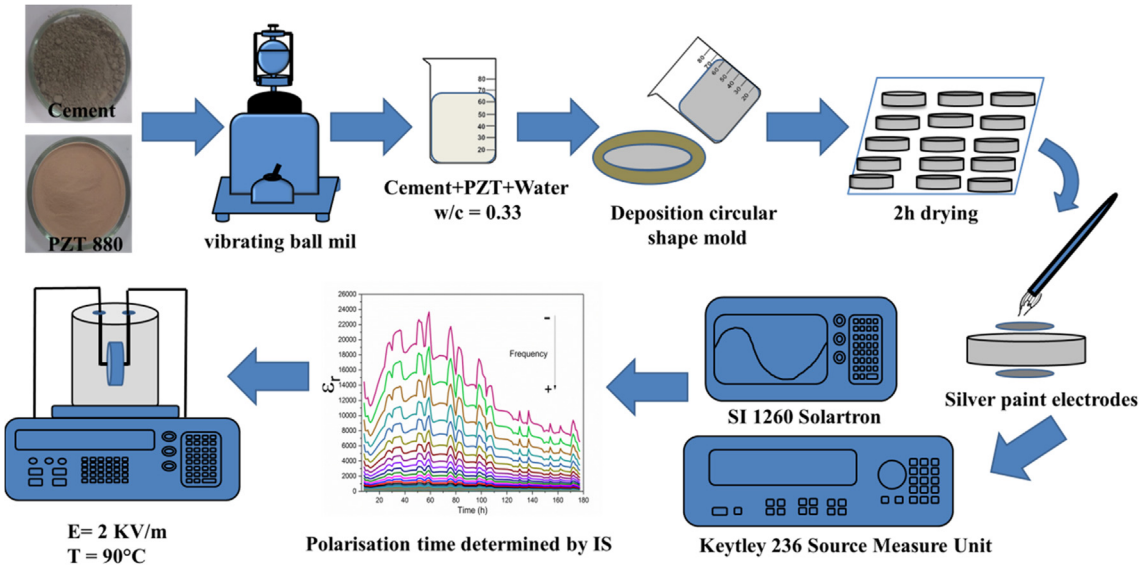

Fig. 1. Schematic representation of the cement-based composite fabrication.

3.2. DC electrical conductivity

The DC electrical conductivity of the cement as a function of the hydration time is shown in Fig. 3. As observed, the measurements were started from eight hours after the beginning of the hydration process, basically characterising the acceleration stage [41-48]. The behaviour shows, as a general profile for the cement sample, a continuous reduction in electrical conductivity values with increasing hydration time, from 1.0×10^{-5} S/m, after eight hours of hydration, to approximately 1.2×10^{-7} S/m after 30 days of curing. This period was basically characterised by the formation of the cement microstructure. During this, there is a transition from a highly interconnected structure of pores, to a segmented one, due to the formation of the hydration products from the curing reaction, which occupy the spaces previously used by the free water which is consumed by this process [49,50]. As the ions can only migrate through capillary pores, their mobility decreases, and consequently, so does the conductivity of the hydrated samples. Furthermore, the consumption (chemical reaction) of the ions in the formation of the hydrated products, and in part, the possible evaporation processes of the water present in the samples, also help in the observed reduction of the conductivity with the hydration time as shown in Fig. 3. It was also observed that although there was a general tendency of electrical conductivity reduction with the cement curing time, the conductivity profile of the hydrated cement presents peaks at different cure intervals. These increases in the conductivity values indicated an increase in the ion concentration in the ionic solution. This allows for an increase in conductivity during specific reaction processes, which may include the formation of new phases related to the presence of delayed hydration processes linked to the presence of unhydrated, or partially hydrated, cement grains, as observed by MEV, or even existing phase transformations such as that of ettringite into monosulphates, during which there is a great release of Ca^{2+} and SO^{2-} [49,50]. Such peaks tended to decrease in intensity as the curing process proceeded over time, indicating a decrease in the curing processes of the cement. For the composites, it was verified that the electrical conductivity reduction, with the increase of the PZT insertion, was attributed to the high insulation characteristic of PZT. Another aspect contributing to this behaviour is the reduction of the ionic contents found in systems with a lower fraction of cement. The general behaviour of the composite's electrical conductivity, as a function of time, showed a gradual reduction which is characteristic of the cement microstructure formation and the consequent interruption of the interconnected pores, a fact previously discussed. However, as seen in Fig. 3, the composite's electrical conductivity, similar to that observed for cement, showed sporadic increases at specific curing intervals. It was verified that such conductivity peaks (inset) coincided, in time period, with those presented by the cement, however, they tended to move for longer curing times with increasing ceramic concentration, thereby indicating a reduction in the cure rate of the cement with the increase of the piezoelectric ceramic contents in the composites. In this way, the PZT has been shown to act as a physical barrier

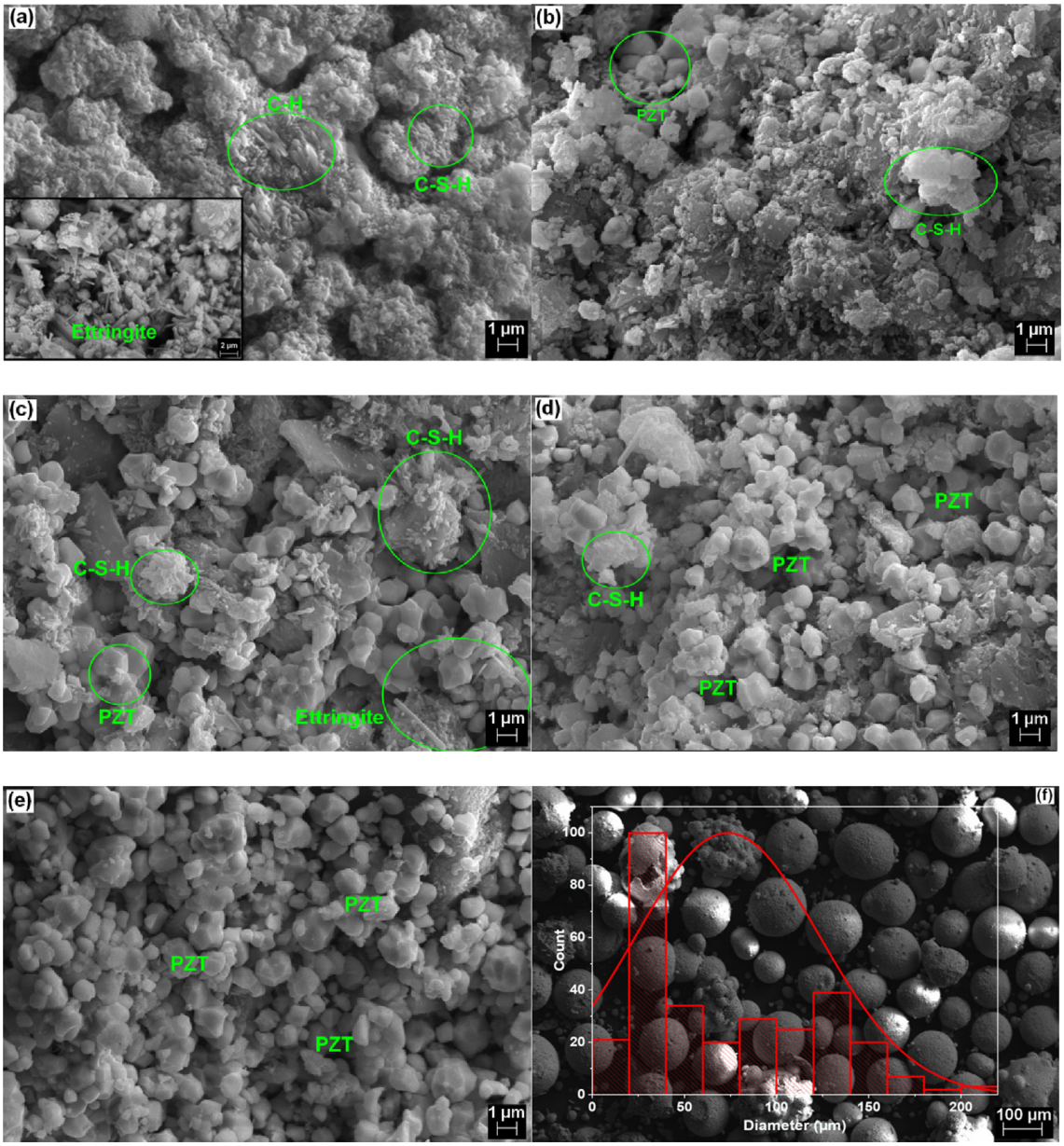

Fig. 2. SEM fracture micrographs by backscattered electrons at 10.000x magnification of (a) cement; Inset shows cement porous image with ettringite presence (b) CP (90/10), (c) CP (70/30), (d) CP (50/50), (e) CP (70/30) at 30 days cure and SEM by secondary electrons for (f) PZT (200x magnification); Inset shows PZT size distribution.

to the ions migration in the solution, and in the course of the hydration process, to increase the tortuosity of the capillary pores, resulting in a rate reduction of the cement curing process, which can be better observed through impedance spectroscopy measurements.

3.3. Impedance spectroscopy

Figs. 4 and 5 shows the values of ε_r as a function of the hydration time, at different frequencies, for cement and the composites, respectively. A typical behaviour of ε_r, reducing with increasing frequency, could be observed for cement (Fig. 4), as a consequence of the inability of some existing polarisation mechanisms in the material to follow the alternation of the applied electric field. Fig. 4 shows that the ε_r cement behavior, as a function of curing time, can be divided in three distinct periods: the first characterised by the interval between 8 and 13 h, in which the dielectric constant values tended to decrease continuously. The second, ranged between 13 and 62 h when ε_r had, as general behaviour, a tendency to increase, and the third period, located after 62 h, when it tended to reduce continuously.

The reduction behaviour of ε_r values up to 13 h of hydration is based on the continuous reduction of the electrode amplification effects, which are more intense in the initial curing periods and tend to decrease as the conduction pathways are reduced with the formation of cement hydration products [51,52]. This is due to the interruption of the conductive pathways formed by the interconnection of the pores and capillaries, due to the formation of the hydration products, as well as the consumption of free water in the system during the curing process, which reduces the possible formation of oxygen in the system so reducing the formation of the insulation layer between the electrode and cement paste [53] After 13 h, a significant amount of hydration products had originated, and the microstructure of the cement interfered in a significant way with the ε_r values of the cement. The interruption

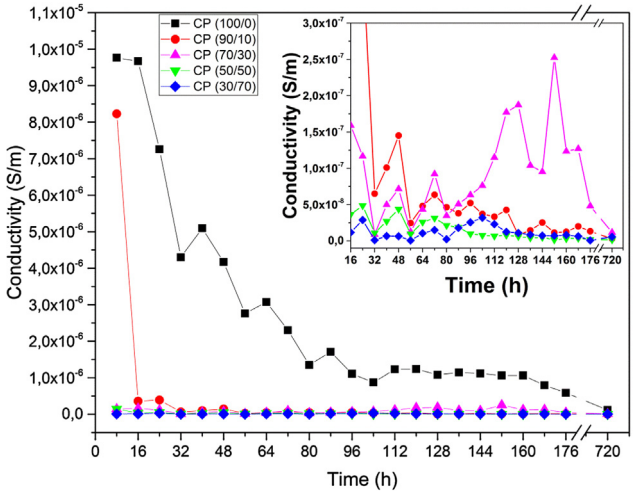

Fig. 3. Electrical conductivity profile of cement and cement-based composites as a function of curing time.

of the capillary pore connection, the formation of disconnected pores, and the effect of the double electric layer formation between the pore fluid and the hydration products, generated interfacial polarisation processes, resulting in an increase in the ε_r values [48,54]. However, as observed in Fig. 4, ε_r showed high values compared to its main constituent phases [48,48,54-56]. Coverdale et al. [48,54] observed a similar process, attributing it to the existence of amplification mechanisms originated by capillary pores that extend throughout the sample geometry, obstructed only by thin insulating barriers. Each channel contributes with an extremely high capacitance in terms of the sample response. In this way, the ε_r reduction tendency, after 62 h, can be attributed to the microstructure change with the formation of the hydration products, due to the consequent capillary pores closure, and/or narrowing, and by the gradual increase of the insulation barriers thickness [48,54]. Also, it was possible to observe in Fig. 4, excluding the general behaviour discussed above, the presence of peaks characterising the increase of the ε_r in specific hydration periods. These peaks have a bandwidth around 5 to 12 h and tended to decrease in intensity with increasing oscillation frequency and cure time. It is believed that these are associated to chemical reaction processes constituted by a large ionic release characteristic of the formation of new phases or transformation of the already existing phases, as observed in the DC conductivity measurements. As the reaction continued and more and more hydrated phases were formed and ions were released, the thin insulation barriers became thicker, pores became discontinuous, and the conductivity was reduced, leading to a reduction of the dielectric constant, characterising the peak in the dielectric spectrum.

In turn, the introduction of increasing fractions of PZT in the composites, in relation to the cement paste, promoted an increase in the values of ε_r, as a consequence of the high dielectric constant presented by the ferroelectric ceramics - Fig. 5(a–d). However, the values of ε_r were below the values determined for PZT or, for the simple model of association of capacitances of the main dielectric phases present (C-S-H, PZT). These values were attributed to the composite's porosity increase, with the PZT introduction, based on the reduction and delay of the hydrated products formation, as well as the low surface adhesion of the hydrated products on the PZT surface, as seen in the SEM images. This behaviour was intensified in situations where the ceramic volumetric fraction tended to promote phase inversion processes, due to the beginning of the percolation, when the PZT dielectric constant dominates the composite bulk behaviour - Fig. 5(c–d). Similar behaviour was observed by Chomyen et al. [20], which verified the high sensitivity of ε_r to interface microstructure variations in three-phase composites of cement/$BaTiO_3$ and fly ash.

In relation to the ε_r composites spectra as a function of the curing time (Fig. 5b–e), these presented a unique behaviour, unlike pure cement, showing a tendency to decrease with increasing frequency. This fact was attributed to the microstructure change with the hydration products formation, as already discussed. However, as can be seen, this reduction behaviour became more accentuated during the initial hydration periods. Furthermore, there was a greater stability of the values of ε_r with an increase of the hydration time and an increase of the ceramic fraction. This factor was attributed to the PZT, which presents a high ε_r stability, as a function of the frequency, compared to the cement.

It was possible to verify high values of ε_r for 10% PZT, compared to its main constituent phases, in the initial periods of hydration at

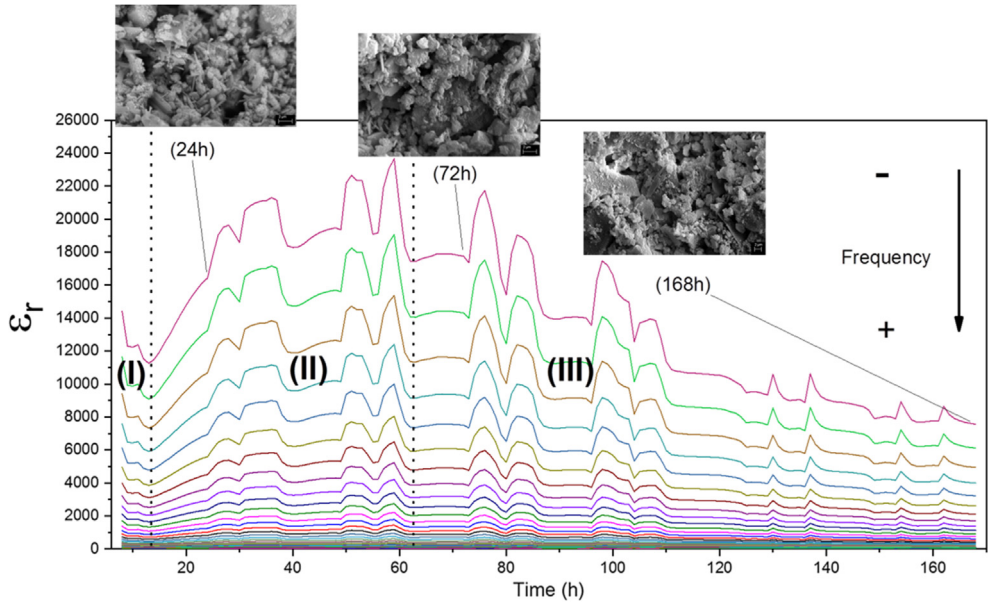

Fig. 4. Dielectric spectra as a function of curing time for cement at different frequencies. Inset shows the fracture micrographs for periods of 24, 72 and 168 h.

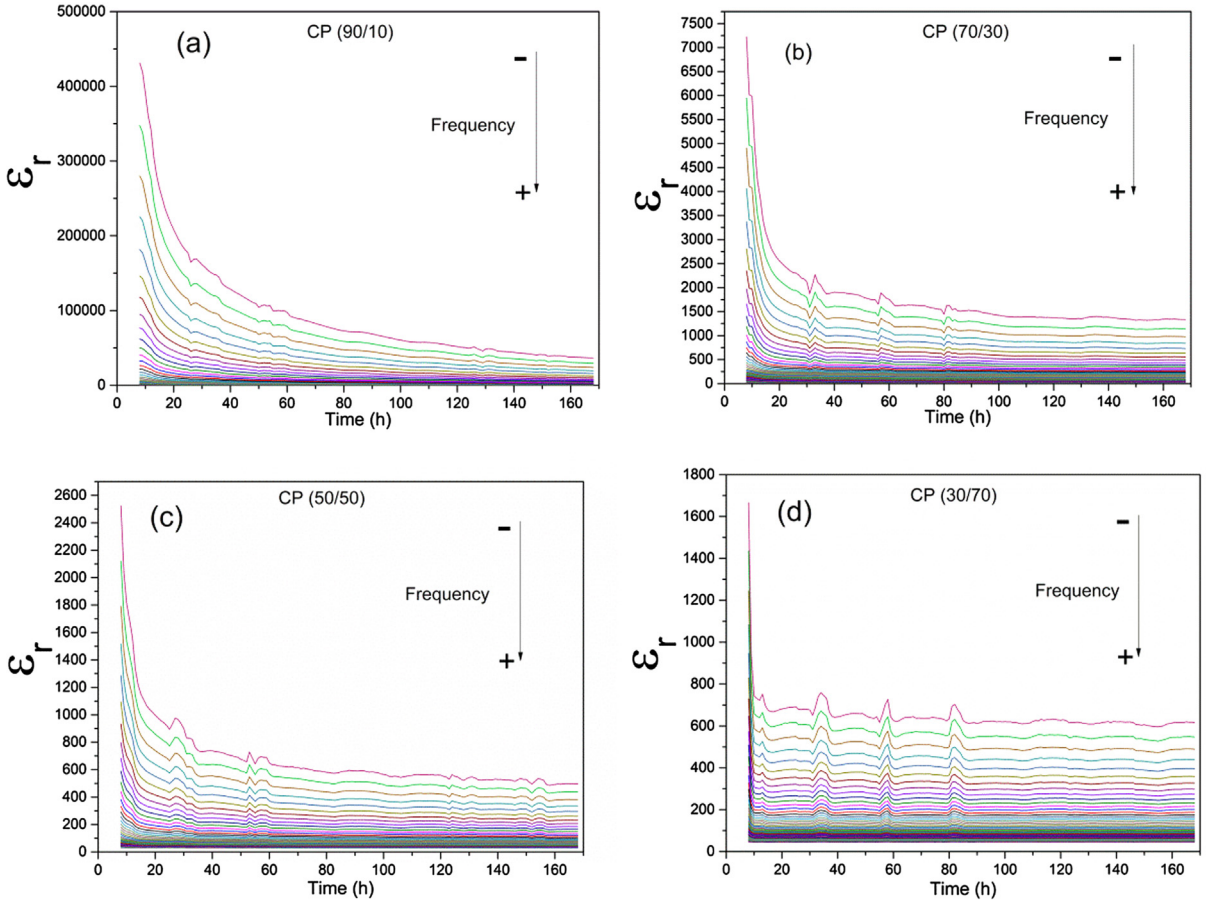

Fig. 5. Dielectric spectra as a function of curing time for cement composites at different frequencies: (a) CP (90/10), (b) CP (70/30), (c) CP (50/50) and (d) (70/30).

intermediate frequencies. These values tended to decrease with increasing PZT concentrations, reaching values close to the main predominant phases in the composite (C-S-H, PZT) [54-56]. Thus, at low PZT concentrations, as observed for cement, dielectric amplification mechanisms, as described by Coverdale et al. [48,54,55], have a great influence on the ε_r amplification. However, as the ceramic fraction increased, the increase in the capillary pores tortuosity and the increase of porosity, both due to the presence of the piezoelectric ceramic, resulted in a reduction of such amplification mechanisms, causing a reduction of the ε_r. Similar to the impedance spectra observed for the cement paste, the composite's spectra showed an ε_r increase at specific curing times coinciding with, or close to, that of the cement. However, such increases are shown as bands for all PZT concentrations. Such bands tended to lose resolution and increase their width with increasing amount of PZT. Also, a small ε_r band displacement at longer curing times, (up to 50 h), with the ceramic particulate introduction, could be observed. Above these periods, no significant displacement was observed. These events are linked to the PZT action as an ion migration barrier, delaying the curing process of the cement paste in the initial hydration stages.

3.4. Piezoelectric coefficient

Fig. 6(a-d) shows the d_{33} composites as a function of the curing age polarisation, measured for 105 days after polarisation. As expected, higher ceramic fractions in the matrix promoted higher values of the d_{33} composites. The piezoelectric coefficient showed an increase with curing time polarisation, followed by a reduced trend for the final period of 30 days. For a biphasic composite, the average piezoelectric coefficient can be expressed as [6,57] :

$$\overline{d_{33}} = \varphi L_t L_e E_l d_1 \quad (1)$$

in which: φ is the ceramic volumetric fraction; d_1 = PZT piezoelectric coefficient; L_t and L_e = local stress, and E_l = local polarisation electric field. The highest values of ε_r were found during the initial cure periods, as already shown. However, the highest obtained value of d_{33} was for the curing period in which the sample was polarised for 130 h. Thus, the observed results are a combination of factors linked to the cement curing process and the ε_r values. In the initial curing stage, the ionic concentration, present in the system, is relatively high, so during the polarisation there was a reduction of the local polarisation electric field over the ceramic grains due to the presence of loss currents [8]. This process was intensified by polarising the samples during periods in which the values of ε_r presented a maximum, categorised by a higher ionic presence in the particular time period. It is also associated with the fact that the presence of pores, in the initial periods of hydration, reduces the mechanical stress transfer to the ceramic grains so justifying the lower values of d_{33} for the periods of 8, 51 and 76 h. The high d_{33} found for composites, after 130 h, is due to the reduction of the loss current by reducing the cement curing process, as well as the reduction in the pores with the curing process. By such reasoning, the higher values of the piezoelectric coefficient should have been observed for the curing age polarisation of 30 days. However, since the values of ε_r in such a period are considerably reduced, the polarisation of the ceramic grains in the cementitious matrix is also reduced, due to the low mobility of free charges.

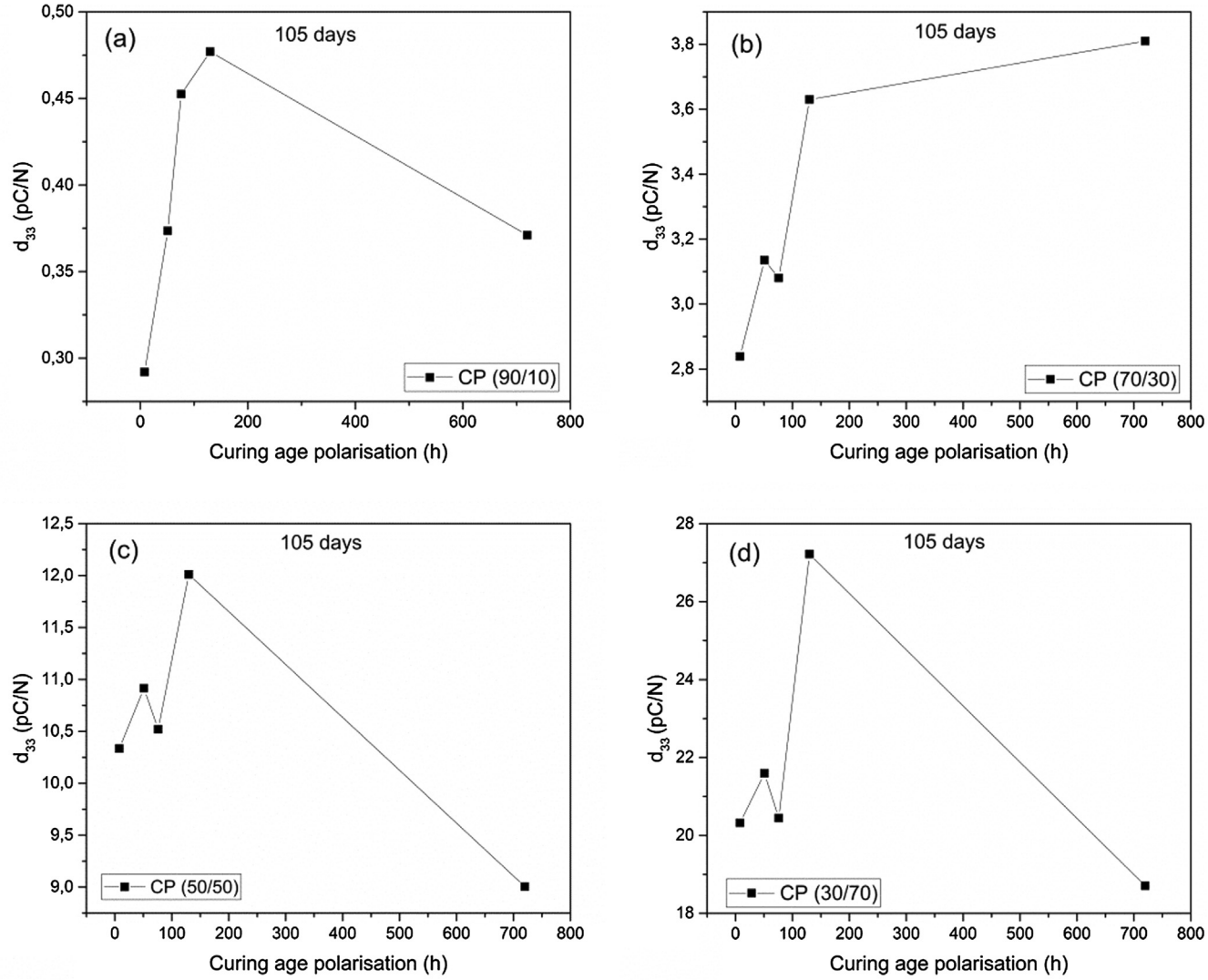

Fig. 6. Composites d_{33} as a function of curing age polarisation measured in 105 days after polarisation.

Fig. 7(a–d) shows d_{33} values as a function of the post-polarisation curing time. Ferroelectric ceramics such as PZT tend to undergo ageing processes after polarisation. This is characterised by the d_{33} reduction with time, resulting from the samples internal stress release, as well as the rearrangement of the ferroelectric domains due to thermodynamic processes [58]. Thus, as shown in Fig. 7(a–d), samples with PZT concentrations equal to, or greater than, 50% v/v showed a typical behaviour of the ferroelectric ceramics, demonstrating a tendency to gradually reduce d_{33} values with the time of measurement/cure. However, for PZT concentrations below 50%, great instability was observed in the piezoelectric coefficient values over time. Such instabilities were higher in the initial curing polarisation periods, as well as in the initial post-polarisation measurement periods. Gong [59] observed similar behaviour in samples of white cement/PZT/carbon black, attributing such behaviour to the cement cure process itself. During the hydration process of the cement, there is a large presence of ions in the system. Some of these ions, present in the ionic solution, can adsorb on the solid surface of the pores by electrostatic interaction. In this way, the formation of dipoles allows their orientation in the presence of the polarising electric field. As these dipoles are less stable than those presented by the ferroelectric ceramics, they tend to revert to their initial post-polarisation configurations, resulting in fluctuations in the piezoelectric coefficient values, and in a great tendency, reductions in the same as observed [59]. However, such processes add to the stress increase in the interfacial regions of the cement/PZT with the cement cure, originates d_{33} peaks over the time, contributing to instability [6,29,32]. Thus, samples at more advanced curing periods used for polarisation, coupled with the reduction in the amount of PZT, showed smaller instabilities due to the lower ionic fraction present, as well as lower morphological changes due to advanced curing.

4. Conclusion

Cement-based composites were made considering a water/cement ratio of 0.33. The composites were characterised by their piezoelectric properties and also by the influence of PZT on the cement curing process. The results showed a direct influence of PZT on the cement curing process, increasing the curing time of the material. Impedance spectroscopy and DC conductivity measurements indicated that late cure reactions of the cement paste directly interfered with the values of the dielectric constant and the electrical conductivity of the composites. Finally, the results of the d_{33} showed great instability in the initial post-polarisation periods,

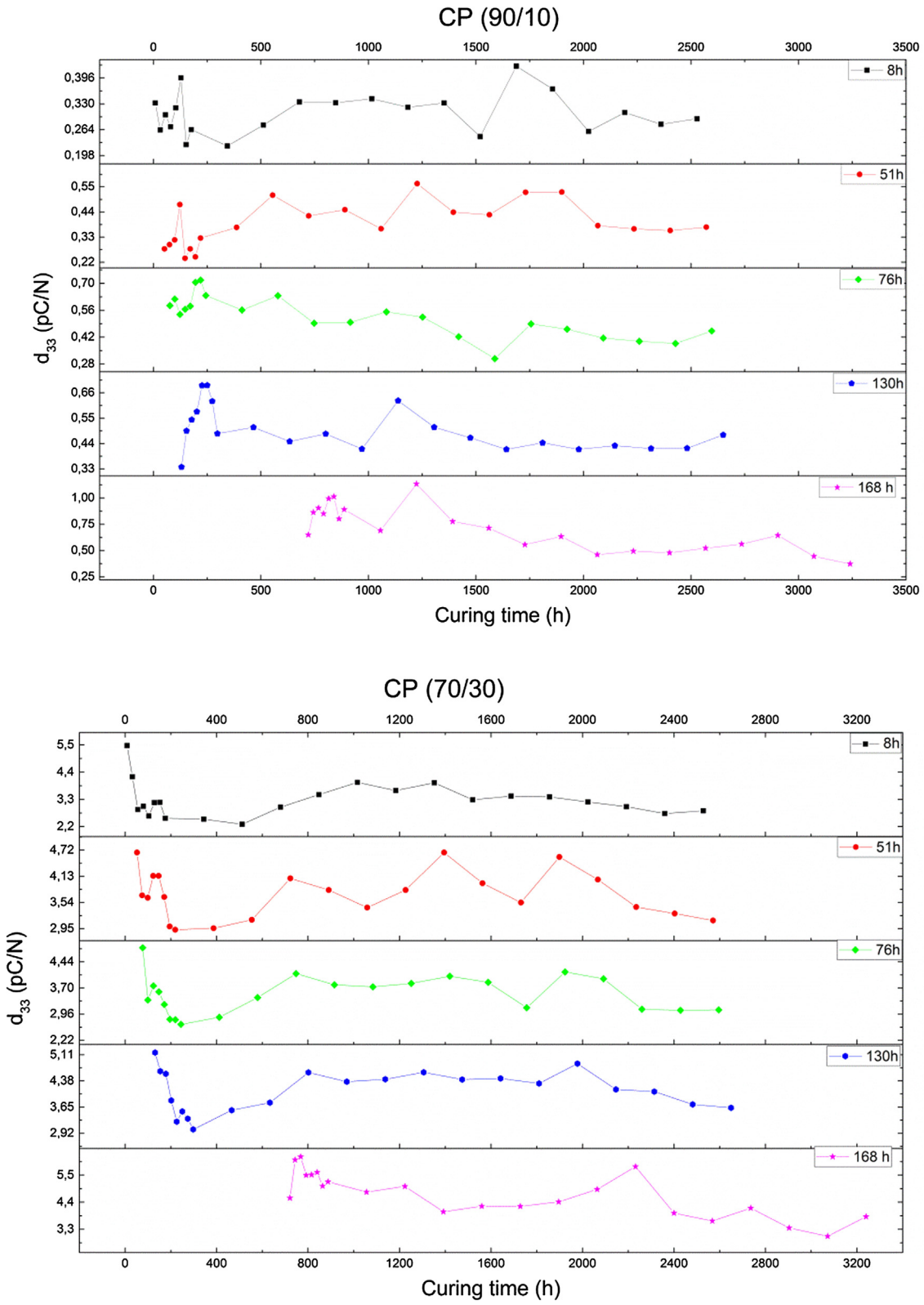

Fig. 7. Piezoelectric coefficient as a function of curing time for different curing age polarisations. Composite's d_{33} was measured, in all cases, until 105 days after polarisation.

for all the compositions, attributed to the existence of unstable dipoles in the samples resulting from the cement curing process. Polarisation, as a function of the curing age, showed an increase in d_{33} values when the samples were polarised at a later cure age, with a maximum for 130 h measured at 105 days after polarisation, and reducing to polarisations carried out in 30 days of cure. Such behaviour was attributed to the cement curing process, and the ε_r values, in such periods.

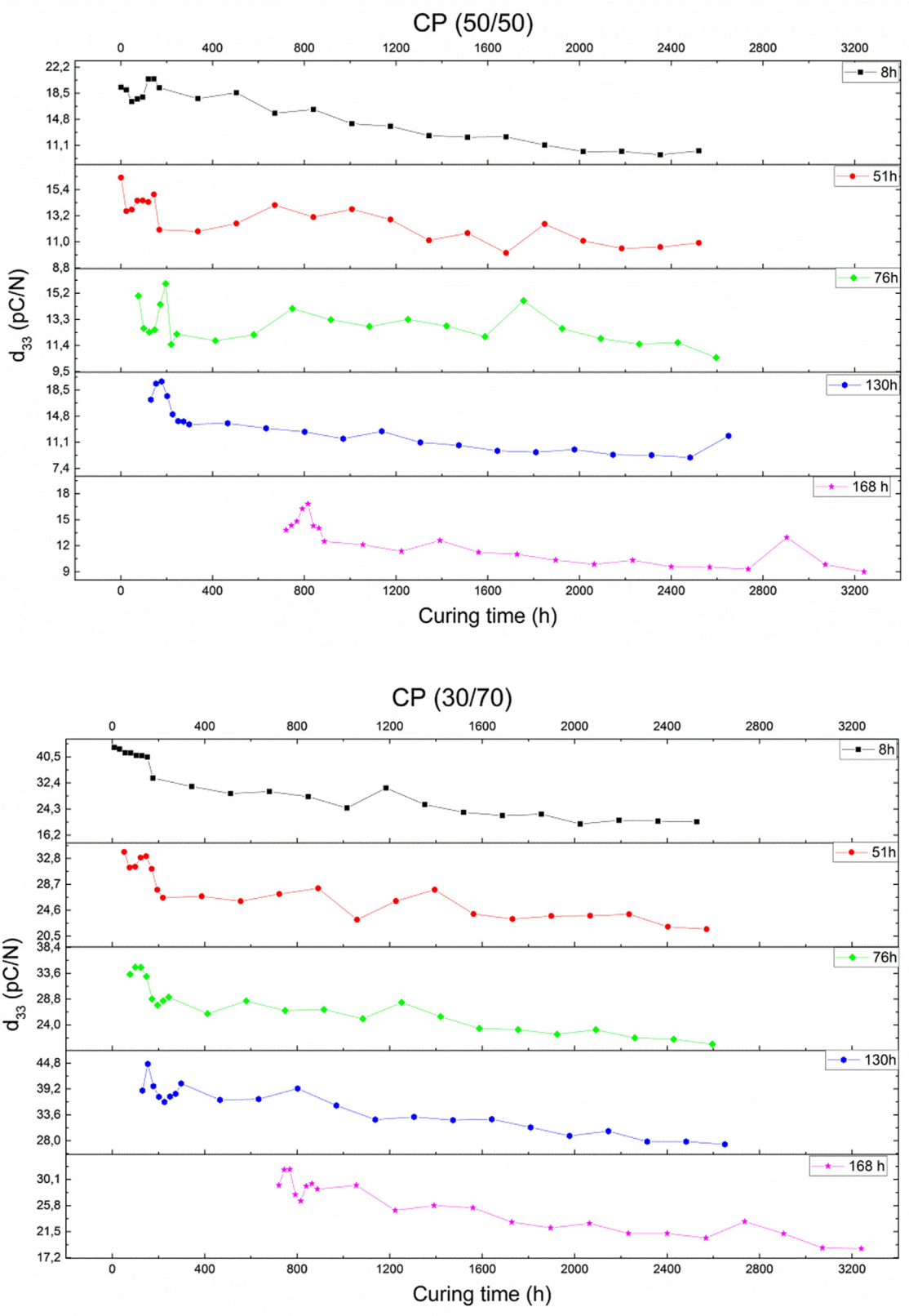

Fig. 7 (*continued*)

CRediT authorship contribution statement

J.A. Santos: Validation, Formal analysis, Investigation, Data curation, Writing - original draft, Writing - review & editing. **A.O. Sanches:** Conceptualization, Methodology, Validation, Formal analysis, Investigation, Data curation, Writing - original draft, Writing - review & editing, Project administration. **J.L. Akasaki:** Formal analysis, Writing - original draft, Writing - review & editing, Supervision. **M.M. Tashima:** Conceptualization, Methodology, Formal analysis, Writing - original draft, Writing - review & editing, Supervision. **E. Longo:** Formal analysis, Resources, Writing - original draft, Funding acquisition. **J.A. Malmonge:** Conceptualization, Methodology, Validation, Formal analysis, Investigation, Resources, Data curation, Writing - original draft, Supervision, Project administration.

Declaration of Competing Interest

The authors declare that they have no known competing financial interests or personal relationships that could have appeared to influence the work reported in this paper.

Acknowledgments

The authors express their gratitude to Fundação de Amparo à Pesquisa do Estado de São Paulo – FAPESP (CEPID – CDMF Grant 2013/07296-2), Coordenação de Aperfeiçoamento de Pessoal de Nível Superior – CAPES (Finance Code 001) and Conselho Nacional de Desenvolvimento Científico e Tecnológico (CNPq), for the financial support and scholarship.

References

[1] J. Chen, Q. Qiu, Y. Han, D. Lau, Piezoelectric materials for sustainable building structures: fundamentals and applications, Renew. Sustain. Energy Rev. 101 (2019) 14–25, https://doi.org/10.1016/j.rser.2018.09.038.
[2] T. Weng, Y. Agarwal, From buildings to smart buildings-sensing and actuation to improve energy efficiency, IEEE Des. Test Comput. 29 (2012) 36–44, https://doi.org/10.1109/MDT.2012.2211855.
[3] S. Roy, H. Mishra, B.G. Mohapatro, Creating sustainable environment using smart materials in smart structures, Indian J. Sci. Technol. 9 (2016), https://doi.org/10.17485/ijst/2016/v9i30/99171.
[4] A. Zanella, N. Bui, A. Castellani, L. Vangelista, M. Zorzi, Internet of things for smart cities, IEEE Internet Things J. 1 (2014) 22–32, https://doi.org/10.1109/JIOT.2014.2306328.
[5] J. Qiu, H. Ji, Research on applications of piezoelectric materials in smart structures, Front. Mech. Eng. 6 (2011) 99–117, https://doi.org/10.1007/s11465-011-0212-4.
[6] C. Xin, H. Shifeng, C. Jun, X. Ronghua, L. Futian, L. Lingchao, Piezoelectric and dielectric properties of piezoelectric ceramic-sulphoaluminate cement composites, J. Eur. Ceram. Soc. 25 (2005) 3223–3228, https://doi.org/10.1016/j.jeurceramsoc.2004.07.031.
[7] G. Song, V. Sethi, H.N. Li, Vibration control of civil structures using piezoceramic smart materials: a review, Eng. Struct. 28 (2006) 1513–1524, https://doi.org/10.1016/j.engstruct.2006.02.002.
[8] A.O. Sanches, G.F. Teixeira, M.A. Zaghete, E. Longo, J.A. Malmonge, M.J. Silva, W. K. Sakamoto, Influence of polymer insertion on the dielectric, piezoelectric and acoustic properties of 1–0-3 polyurethane/cement-based piezo composite, Mater. Res. Bull. 119 (2019), https://doi.org/10.1016/j.materresbull.2019.110541 110541.
[9] R. Rianyoi, R. Potong, N. Jaitanong, R. Yimnirun, A. Chaipanich, Dielectric, ferroelectric and piezoelectric properties of 0–3 barium titanate-Portland cement composites, Appl. Phys. A Mater. Sci. Process. 104 (2011) 661–666, https://doi.org/10.1007/s00339-011-6307-2.
[10] H.H. Pan, C.K. Wang, Y.C. Cheng, Curing time and heating conditions for piezoelectric properties of cement-based composites containing PZT, Constr. Build. Mater. 129 (2016) 140–147, https://doi.org/10.1016/j.conbuildmat.2016.10.107.
[11] Z. Li, D. Zhang, K. Wu, Cement-Based 0–3 Piezoelectric Composites, J. Am. Ceram. Soc. 85 (2002) 305–313.
[12] H.H. Pan, D.H. Lin, R.H. Yang, High piezoelectric and dielectric properties of 0–3 PZT/cement composites by temperature treatment, Cem. Concr. Compos. 72 (2016) 1–8, https://doi.org/10.1016/j.cemconcomp.2016.05.025.
[13] R. Potong, R. Rianyoi, A. Ngamjarurojana, A. Chaipanich, Microstructure and performance of 1–3 connectivity environmental friendly lead-free BNBK-Portland cement composites, Mater. Res. Bull. 90 (2017) 59–65, https://doi.org/10.1016/j.materresbull.2017.02.008.
[14] X. Cheng, D. Xu, L. Lu, S. Huang, M. Jiang, Performance investigation of 1–3 piezoelectric ceramic-cement composite, Mater. Chem. Phys. 121 (2010) 63–69, https://doi.org/10.1016/j.matchemphys.2009.12.045.
[15] R. Han, Z. Shi, Y.L. Mo, Static analysis of 2–2 cement-based piezoelectric composites, Arch. Appl. Mech. 81 (2011) 839–851, https://doi.org/10.1007/s00419-010-0454-3.
[16] T. Zhang, Y. Liao, W. Liu, Theoretical solutions of 2–2 multi-layered cement-based piezoelectric composite under impact load, Compos. Struct. 195 (2018) 249–264, https://doi.org/10.1016/j.compstruct.2018.04.059.
[17] X. Dongyu, C. Xin, H. Shifeng, Investigation of inorganic fillers on properties of 2–2 connectivity cement/polymer based piezoelectric composites, Constr. Build. Mater. 94 (2015) 678–683, https://doi.org/10.1016/j.conbuildmat.2015.07.090.
[18] D. Zou, C. Du, T. Liu, W. Li, Effects of temperature on the performance of the piezoelectric-based smart aggregates active monitoring method for concrete structures, Smart Mater. Struct. (2019) 1–16, https://doi.org/10.1088/1361-665X/aafe15.
[19] M. Lezgy-Nazargah, S. Saeidi-Aminabadi, M.A. Yousefzadeh, Design and fabrication of a new fiber-cement-piezoelectric composite sensor for measurement of inner stress in concrete structures, Arch. Civ. Mech. Eng. 19 (2019) 405–416, https://doi.org/10.1016/j.acme.2018.12.007.
[20] P. Chomyen, R. Potong, R. Rianyoi, A. Ngamjarurojana, P. Chindaprasirt, A. Chaipanich, Microstructure, dielectric and piezoelectric properties of 0–3 lead free barium zirconate titanate ceramic-Portland fly ash cement composites, Ceram. Int. 44 (2018) 76–82, https://doi.org/10.1016/j.ceramint.2017.09.112.
[21] E. Ghafari, Y. Yuan, C. Wu, T. Nantung, N. Lu, Evaluation the compressive strength of the cement paste blended with supplementary cementitious materials using a piezoelectric-based sensor, Constr. Build. Mater. 171 (2018) 504–510, https://doi.org/10.1016/j.conbuildmat.2018.03.165.
[22] R. Potong, R. Rianyoi, A. Ngamjarurojana, A. Chaipanich, Influence of carbon nanotubes on the performance of bismuth sodium titanate-bismuth potassium titanate-barium titanate ceramic/cement composites, Ceram. Int. 43 (2017) S75–S78, https://doi.org/10.1016/j.ceramint.2017.05.225.
[23] R. Rianyoi, R. Potong, A. Ngamjarurojana, A. Chaipanich, Poling effects and piezoelectric properties of PVDF-modified 0–3 connectivity cement-based/lead-free 0.94(Bi0.5Na0.5)TiO3–0.06BaTiO3 piezoelectric ceramic composites, J. Mater. Sci. 53 (2018) 345–355, https://doi.org/10.1007/s10853-017-1533-4.
[24] N.A. Soliman, K.H. Khayat, M. Karray, A.F. Omran, Piezoelectric ring actuator technique to monitor early-age properties of cement-based materials, Cem. Concr. Compos. 63 (2015) 84–95, https://doi.org/10.1016/j.cemconcomp.2015.09.001.
[25] S. Banerjee, J. Torres, K.A. Cook-Chennault, Piezoelectric and dielectric properties of PZT-cement-Aluminum nano-composites, Ceram. Int. 41 (2014) 819–833, https://doi.org/10.1016/j.ceramint.2014.05.136.
[26] B. Dong, Y. Liu, N. Han, H. Sun, F. Xing, D. Qin, Study on the microstructure of cement-based piezoelectric ceramic composites, Constr. Build. Mater. 72 (2014) 133–138, https://doi.org/10.1016/j.conbuildmat.2014.08.058.
[27] B. Dong, Z. Li, Cement-based piezoelectric ceramic smart composites, Compos. Sci. Technol. 65 (2005) 1363–1371, https://doi.org/10.1016/j.compscitech.2004.12.006.
[28] M. Sun, Z. Li, X. Song, Piezoelectric effect of hardened cement paste, Cem. Concr. Compos. 26 (2004) 717–720, https://doi.org/10.1016/S0958-9465(03)00104-5.
[29] Z. Li, B. Dong, D. Zhang, Influence of polarization on properties of 0–3 cement-based PZT composites, Cem. Concr. Compos. 27 (2005) 27–32, https://doi.org/10.1016/j.cemconcomp.2004.02.001.
[30] S. Huang, X. Li, F. Liu, J. Chang, D. Xu, X. Cheng, Effect of carbon black on properties of 0–3 piezoelectric ceramic/cement composites, Curr. Appl Phys. 9 (2009) 1191–1194, https://doi.org/10.1016/j.cap.2009.01.011.
[31] S. Hunpratub, T. Yamwong, S. Srilomsak, S. Maensiri, P. Chindaprasirt, Effect of particle size on the dielectric and piezoelectric properties of 0–3BCTZO/cement composites, Ceram. Int. 40 (2014) 1209–1213, https://doi.org/10.1016/j.ceramint.2013.05.118.
[32] A. Chaipanich, R. Rianyoi, R. Potong, N. Jaitanong, Aging of 0–3 piezoelectric PZT ceramic-Portland cement composites, Ceram. Int. 40 (2014) 13579–13584, https://doi.org/10.1016/j.ceramint.2014.05.073.
[33] S.W. Tang, X.H. Cai, Z. He, W. Zhou, H.Y. Shao, Z.J. Li, T. Wu, E. Chen, The review of pore structure evaluation in cementitious materials by electrical methods, Constr. Build. Mater. 117 (2016) 273–284, https://doi.org/10.1016/j.conbuildmat.2016.05.037.
[34] S.W. Tang, X.H. Cai, Z. He, W. Zhou, H.Y. Shao, Z.J. Li, T. Wu, E. Chen, The review of early hydration of cement-based materials by electrical methods, Constr. Build. Mater. 146 (2017) 15–29, https://doi.org/10.1016/j.conbuildmat.2017.04.073.
[35] X. Hu, C. Shi, X. Liu, J. Zhang, G. de Schutter, A review on microstructural characterization of cement-based materials by AC impedance spectroscopy, Cem. Concr. Compos. 100 (2019) 1–14, https://doi.org/10.1016/j.cemconcomp.2019.03.018.
[36] M. Cabeza, P. Merino, A. Miranda, X.R. Nóvoa, I. Sanchez, Impedance spectroscopy study of hardened Portland cement paste, Cem. Concr. Res. 32 (2002) 881–891, https://doi.org/10.1016/S0008-8846(02)00720-2.
[37] Y.M. Kim, J.H. Lee, S.H. Hong, Study of alinite cement hydration by impedance spectroscopy, Cem. Concr. Res. 33 (2003) 299–304, https://doi.org/10.1016/S0008-8846(02)00944-4.

[38] M. Cabeza, M. Keddam, X.R. Nóvoa, I. Sánchez, H. Takenouti, Impedance spectroscopy to characterize the pore structure during the hardening process of Portland cement paste, Electrochim. Acta 51 (2006) 1831–1841, https://doi.org/10.1016/j.electacta.2005.02.125.
[39] S.W. Tang, Z.J. Li, E. Chen, H.Y. Shao, Impedance measurement to characterize the pore structure in Portland cement paste, Constr. Build. Mater. 51 (2014) 106–112, https://doi.org/10.1016/j.conbuildmat.2013.10.064.
[40] F. He, R. Wang, C. Shi, R. Zhang, C. Chen, L. Lin, X. An, Differential analysis of AC impedance spectroscopy of cement-based materials considering CPE behavior, Constr. Build. Mater. 143 (2017) 179–188, https://doi.org/10.1016/j.conbuildmat.2017.03.119.
[41] X. Wei, Z. Li, Early hydration process of portland cement paste by electrical measurement, J. Mater. Civ. Eng. 18 (2006) 99–105, https://doi.org/10.1061/(ASCE)0899-1561(2006) 18:1(99).
[42] Z. Li, L. Xiao, X. Wei, Determination of concrete setting time using electrical resistivity measurement, J. Mater. Civ. Eng. 19 (2007) 423–427, https://doi.org/10.1061/(ASCE)0899-1561(2007) 19:5(423).
[43] G. Levita, A. Marchetti, G. Gallone, A. Princigallo, G.L. Guerrini, Electrical properties of fluidified Portland cement mixes in the early stage of hydration, Cem. Concr. Res. 30 (2000) 923–930, https://doi.org/10.1016/S0008-8846(00)00282-9.
[44] A. Princigallo, K. Van Breugel, G. Levita, Influence of the aggregate on the electrical conductivity of Portland cement concretes, Cem. Concr. Res. 33 (2003) 1755–1763, https://doi.org/10.1016/S0008-8846(03)00166-2.
[45] S.W. Tang, Z.J. Li, H.Y. Shao, E. Chen, Characterization of early-age hydration process of cement pastes based on impedance measurement, Constr. Build. Mater. 68 (2014) 491–500, https://doi.org/10.1016/j.conbuildmat.2014.07.009.
[46] S.W. Tang, X.H. Cai, Z. He, H.Y. Shao, Z.J. Li, E. Chen, Hydration process of fly ash blended cement pastes by impedance measurement, Constr. Build. Mater. 113 (2016) 939–950, https://doi.org/10.1016/j.conbuildmat.2016.03.141.
[47] W. Shengnian, W.E.I. Xiaosheng, F.A.N. Zhihong, The early hydration characteristics of portland cements with superplasticizer using electrical measurements, Am. J. Civ. Eng. Archit. 4 (2016) 153–158, https://doi.org/10.12691/ajcea-4-5-1.
[48] R.T. Coverdale, B.J. Christensen, T.O. Mason, H.M. Jennings, E.J. Garboczi, Interpretation of the impedance spectroscopy of cement paste via computer modelling, J. Mater. Sci. 29 (1994) 4984–4992, https://doi.org/10.1007/BF01151088.
[49] I.B. Topu, T. Uygunolu, I. Hocaolu, Electrical conductivity of setting cement paste with different mineral admixtures, Constr. Build. Mater. 28 (2012) 414–420, https://doi.org/10.1016/j.conbuildmat.2011.08.068.
[50] M.G.A. El Wahed, E.E. Hekal, Electrical conductivity of cement pastes in different curing media, J. Mater. Sci. Lett. 8 (1989) 875–878, https://doi.org/10.1007/BF01729931.
[51] N.E.H. Iii, Monitoring of cement hydration by broadband time-domain-reflectometry dielectric spectroscopy, J. Appl. Phys. 96 (2004) 5117–5128, https://doi.org/10.1063/1.1797549.
[52] S.J. FordT, O. MasonB, J. ChristensenR, T. CoverdaleH, M. JenningsE, J. Garboczi, Electrode configurations and impedance spectra of cement pastes, J. Mater. Sci. 30 (1994) 1217–1224, https://doi.org/10.1007/BF00356122.
[53] P.R. Camp, S. Bilotta, Dielectric properties of portland cement paste as a function of time since mixing, J. Appl. Phys. 66 (1989) 6007–6013, https://doi.org/10.1063/1.343577.
[54] R.T. Coverdale, B.J. Christensen, T.O. Mason, H.M. Jennings, E.J. Garboczi, Interpretation of the impedance spectroscopy of cement paste via computer modelling - Part II Dielectric response, J. Mater. Sci. 29 (1994) 4984–4992, https://doi.org/10.1007/BF01151088.
[55] R.T. Coverdale, E.J. Garboczi, H.M. Jennings, B.J. Christensen, T.O. Mason, Computer simulation of impedance spectroscopy in two dimensions: application to cement paste, J. Am. Ceram. Soc. 76 (1993) 1513–1520, https://doi.org/10.1111/j.1151-2916.1993.tb03933.x.
[56] P. Xie, P. Gu, Z. Xu, J.J. Beaudoin, A rationalized A.C. impedence model for microstructural characterization of hydrating cement systems, Cem. Concr. Res. 23 (1993) 359–367, https://doi.org/10.1016/0008-8846(93)90101-E.
[57] H.G. Lee, H.G. Kim, Influence of microstructure on the dielectric and piezoelectric properties of lead zirconate-polymer composites, J. Am. Ceram. Soc. 72 (1989) 938–942, https://doi.org/10.1111/j.1151-2916.1989.tb06248.x.
[58] Jiashi Yang, in: An Introduction to the Theory of Piezoelectricity, Springer US, 2004, https://doi.org/10.1007/b101799.
[59] H. Gong, Z. Li, Y. Zhang, R. Fan, Piezoelectric and dielectric behavior of 0–3 cement-based composites mixed with carbon black, J. Eur. Ceram. Soc. 29 (2009) 2013–2019, https://doi.org/10.1016/j.jeurceramsoc.2008.11.014.